On the other hand the situation is similar to other high-tech facilities where the cumulative presence of combustible materials is quite high and presents a large hazard, but the probability of ignition is kept low. Strict measure in that regard are taken in the protection of electrical circuitry.

Detection and Suppression

Incipient detection is planned for all interior spaces within the detector and overhead spaces immediately above it. An aspiration, sample-draw smoke detection system is envisaged for the different internal layers with consideration for natural openings, access ways for maintenance and loadings of combustible materials. Maximum advantage will be taken from early warnings, assisted by sophisticated computer systems and a multi-stage adequate response, starting locally. The diversity and redundance of detector systems on the one hand and the screening out of false alarms on the other is still under study. A complicating factor is the replacement of Halon 1211 and 1301, which are ozone depletants. Promising alternatives are being investigated, mainly based on fine mists of water, CO_2 and nitrogen. In the event of a fire incident during accelerator operations, the beam will be aborted and machine interlocks will be broken to allow immediate access for intervention by the safety services. Certain shutdowns will have to be automatic, to switch off electrical supplies which may be a cause or suffer dangerous effects. Ventilation of smoke will precede the preparation of extinguishing and recovery measures as well as easing egress. The simulation of credible fire development scenarios with realistic combustible materials may, however, be necessary to determine quantities of smoke, ventilation rates, environmental aspects for the outside and fresh supplies of oxygen and wind (also as a fire promoter).

6.9.7 Lasers for alignment

The laser-based positioning system is operated with low-energy lasers (35 mW) in the visible light range towards the infrared range. At present HeNe lasers are considered and their placement is such that light tightness is ensured.

6.9.8 Estimate of induced radioactivity

At the LHC we will be confronted with two main mechanisms which induce radioactivity in materials: low energy neutron activation and inelastic hadronic interactions at high energy. Of these the latter will dominate, unless the choice of materials is very unfortunate with respect to neutron activation. Two materials have been identified in the Tracker region, which have high thermal neutron activation cross sections:

- ^{197}Au, contained to 100% in the gold strips of the MSGC detectors, has a thermal neutron capture cross-section of 10^5 mb. The resulting ^{198}Au has a half-life of 2.7 days.
- ^{186}W, contained to 30% in the tungsten of the ECAL crystals. The thermal neutron cross-section is 3.8×10^4 mb and the resulting ^{187}W has a half-life of 24 h. The other tungsten isotopes also have relatively large thermal capture cross sections, but if the isotope abundance, the activation cross sections and gamma intensities of the resulting radionuclides are considered together, ^{186}W is the most significant.

Both of these isotopes have relatively short half-lifes so they will have decayed substantially by the time the CMS endcap has been opened to allow access to the vicinity of the ECAL or the Tracker.

Thus we expect that the dominant component for the activation of the ECAL and the Tracker comes from high energy hadronic interactions. A proper treatment of induced radioactivity requires to establish a full inventory of all created radionuclides and to follow the time dependence of this set of nuclides. The enormous amount of different radionuclides produced in the $PbWO_4$ crystals makes explicit accounting for all of them difficult but facilitates some simple averaging procedures. The Tracker materials are typically very light so that it is feasible to identify the few nuclides which are radiologically significant. For target materials with $A < 30$ the dominant long lived nuclides are ^{7}Be and ^{22}Na.

Two opening scenarios are foreseen for the CMS detector. During the long shut-down the endcap moves far away from the Tracker but in the intermediate technical stop the opening is only a few metres. Thus the induced activity in the endcap ECAL is likely to give an important contribution to the dose equivalent which a person working at the Tracker end-flange would receive. In order to determine safe access, shielding requirements and access times, we need to consider both, the activation of the endcap ECAL and of the Tracker.

6.9.8.1 Induced activity in the ECAL

For heavy target materials, like the ECAL, the large number of different radionuclides produced allows the use of so called ω-factors [6-35]. These are based on the fact that effects due to individual nuclides are averaged out so that the rate of inelastic hadronic interactions (stars) in the material is directly proportional to the gamma emission rate from that material due to the activity induced in it. In the spirit of this average treatment the decay of the dose rate ($\dot{D}$) can be parameterised with the the Overton–Sullivan formula [6-36]

$$\dot{D} \sim \Phi \ln \frac{t_i + t_c}{t_c} \, , \tag{6.2}$$

where t_i is the duration of the irradiation, t_c is the time since the end of the irradiation and Φ is the activating hadron fluence.

A plot of this time-dependence for the assumed LHC operating schedule is shown in Fig. 6.50. We clearly see the three 60-day operating periods per year, separated by 14 day stops and followed by a longer shut-down. It must be emphasised that the dose for $t_c = 0$ cannot be obtained from Eq. (6.2), which reflects the fact that short-lived nuclides are excluded from the parameterisation. The dose during irradiation, shown in Fig. 6.50, corresponds to $t_c = 1$ h. The most important observation is that after the fast drop during the first day of cooling, a further decrease of induced radioactivity is very slow. Except for the low luminosity start-up phase the dose rate at any instant of time is within a factor of three from the dose rate scaled to $t_i = 60$ days and $t_c = 1$ day. In addition this scaling provides the best value for an access a few days after machine stop when the LHC has been operating long enough so that the activity has reached the saturation level.

Figure 6.51 shows the dose rate expected from the CMS Calorimeters after 60 days of irradiation and one day of cooling. Details of the calculation can be found in the safety chapter of the CMS ECAL TDR [6-37]. The Tracker and the beam pipe, have been excluded from this calculation. We can observe doses of the order of 200–300 μSv/h. A safety margin of at least two should be added, which means that we have to design shielding and plan access in view of dose equivalent rates of the order of 0.5 mSv/h in the high-η region of the endcap calorimeters. Following the general trend of the activating hadron fluence in the detector, the dose equivalent rates at larger radii are substantially lower.

6.9.8.2 Induced activity in the Tracker

The simulation methods used to determine the activity of various Tracker modules are described in Section A.7.8. We consider the contact dose rate with typical Tracker elements like detectors, support structures and cooling pipes. The large variety of objects with different shapes prevents

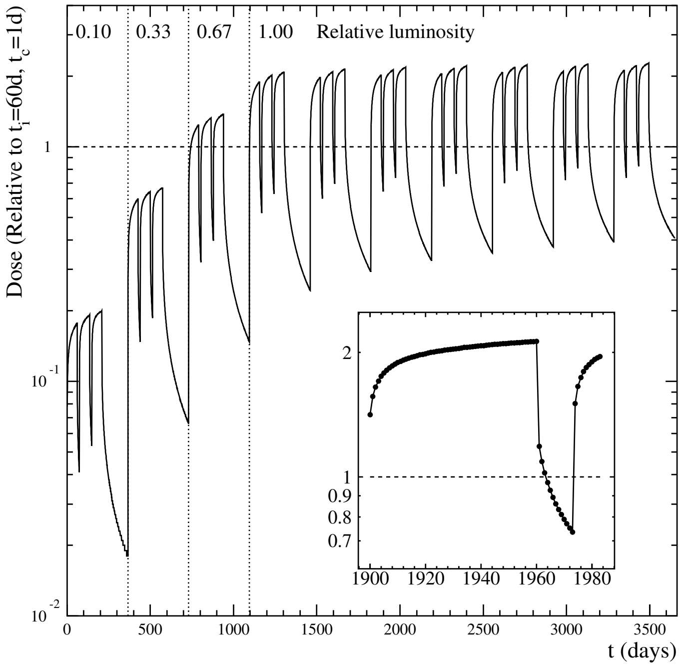

Fig. 6.50: Time variation of induced activity dose rate at the LHC according to the Overton–Sullivan formula. The curve is normalised such that unity (dashed line) coincides with $t_i = 60$ days and $t_c = 1$ day and the maximum average luminosity of LHC (5×10^{33} cm^{-2}s^{-1}). This corresponds to the scaling which is used to present the dose rates in Fig. 6.51. In the small sub-plot the dots indicate individual days.

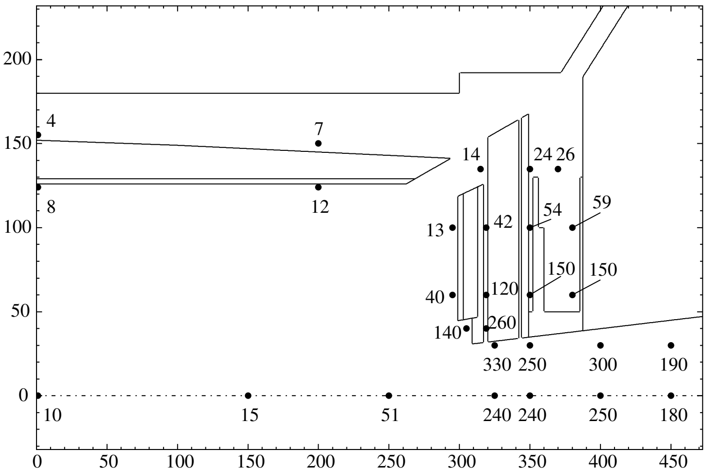

Fig. 6.51: Estimated dose rate in μSv/h around the CMS central calorimeters due to induced radioactivity after $t_i = 60$ days and $t_c = 1$ day (see Fig. 6.50). The average luminosity during the irradiation is assumed to be 5×10^{33} cm^{-2}s^{-1}.

a detailed assessment of the dose for all of them. Thus only some characteristic cases are calculated explicitly.

Of the Tracker materials silicon and aluminium are activated with very similar cross-sections so they can be used as representations of each other [6-38]. Carbon fibre is a good representation for all plastics. Water is introduced to represent the cooling fluids. Iron is used to study the activation of the stainless steel cooling pipes and parts of the beam pipe, but iron activation also gives a good indication for the effects to be expected from copper cables.

The photon dose is calculated by using the emitted energy per unit of volume and scaling it with $0.031\,\mathrm{cm}^2\,\mathrm{g}^{-1}$, which is a good representation of the mass-energy absorption coefficient of tissue over the typical energy range of induced activity photons [6-39]. Figure 6.52 shows the energy emitted in the form of photons for aluminium and iron as a function of cooling time and distance from the beam line. These data form the input for the following estimations of γ-dose rate, the aluminium being treated as representative of silicon and MSGC glass substrates.

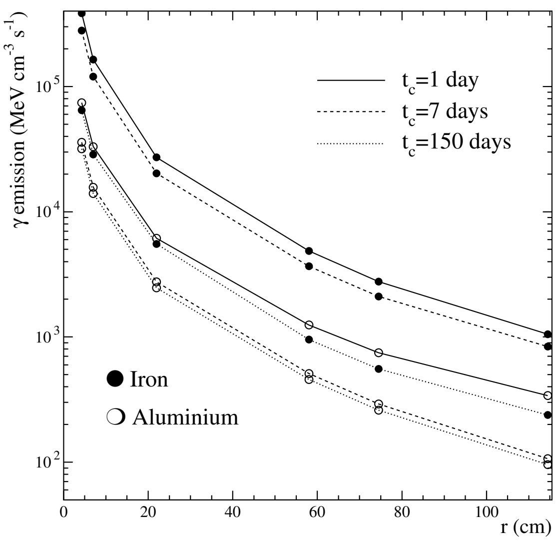

Fig. 6.52: Specific energy emission for aluminium and iron activated at different radii of the Tracker. The values correspond to the end of the tenth year at the LHC and to the indicated cooling time t_c.

The estimation of β dose rate is more complicated due to the large attenuation in materials. A simple estimate can be constructed by assuming the active layer to be infinitely thick so that the dose rate in contact with the surface corresponds to half of the energy emitted per unit of volume in the active material. A detailed simulation of the transport of ^{22}Na β's in a $300\,\mu$m thick silicon plate surrounded by tissue equivalent material shows that the semi-infinite medium assumption decribed above reproduces correctly the dose at the silicon/tissue boundary and overestimates the dose at $70\,\mu$m depth in tissue by a factor of 1.5.

Activation of the detectors

The Pixel detectors are modelled as $600\,\mu$m thick silicon plates in order to include both the sensitive volume and the chips on top of the detectors. A Silicon strip detector is represented by $300\,\mu$m thick plates, i.e. the electronics is not included. For the MSGCs we assume $300\,\mu$m silicon to represent the glass substrate. The drift plane will be carbon-fibre-like material where the activation is negligible compared to the substrate. The activation in the gold strips is significant for the γ dose from the MSGCs, but can be neglected for the β dose rate, since the strips are shielded by the substrate. For the calculation of β contact dose rates all materials are assumed to be semi-infinite. While the γ dose rate is equal on both sides of a complete MSGC module, the β dose rate on the substrate side can be assumed to be negligible.

An inspection of the isotopes produced reveals that, after the first few days of cooling, only ^{22}Na contributes to the dose rate. Thus the dominant uncertainty of the dose estimates given in Table 6.31 comes from the assumed production cross-section of ^{22}Na. A comparison of the prediction of FLUKA [6-40] event generators with experimental data indicates that FLUKA predicts by a factor of 2–3 lower ^{22}Na production. But also the experimental data suffer from significant uncertainties, since only for protons are sufficient data available. Thus the important pion contribution has to be estimated from the proton data, except for a narrow range at few hundred MeV, where some pion activation data are available. The values given in Table 6.31, which are based on the experimental cross-sections, are about a factor of 2 higher than the FLUKA estimates.

It should be emphasised that the γ dose rates given in Table 6.31 apply only to individual modules when removed from the Tracker. While fixed to the Tracker the contribution from all other modules increases the γ dose.

Table 6.31: Estimated contact dose rates (μSv/h) for individual barrel Tracker modules after 10 years of LHC operation. The β-dose rate estimate corresponds to the skin surface. The γ dose rates correspond to 1 mm distance at the centre of a 10×10 cm^2 module. At this distance the dependence on the area is small

Radius	Dose type	t_c=1 day	t_c=7 days	t_c=30 days	t_c=150 days
4.3 cm	γ	69	33	33	30
	β	440	170	160	150
7.1 cm	γ	31	15	14	13
	β	200	73	72	66
22 cm	γ	3.1	1.4	1.3	1.2
	β	37	13	13	12
58 cm	γ	0.62	0.25	0.25	0.23
	β	7.7	2.4	2.4	2.2
74.5 cm	γ	1.0	0.25	0.14	0.13
	β	4.6	1.4	1.3	1.2
114.5 cm	γ	0.81	0.16	0.052	0.048
	β	2.2	0.5	0.49	0.45

Activation of the cooling pipes

The cooling pipes are proposed to be either aluminium or stainless steel. Since an individual pipe is a thin object and the geometry of the pipework is complicated, it does not appear feasible to provide estimates of contact dose rates. The contact dose rates given for the detector modules in Table 6.31 give a relatively good indication of the dose to be expected from a group of cooling pipes. The relative differences of steel and aluminium can be deduced from Fig. 6.52, where it can be seen that the difference between these two materials depends on the cooling time. The difference reaches a maximum after about one week of cooling time but thereafter decreases with increasing t_c. A fairly good general approximation is, however, that steel and aluminium give equal dose rate per unit of mass.

Activation of the support structure

The support structures are assumed to be all carbon fibre. There are no radiologically significant long-lived nuclides which could be produced in carbon-fibre composites[2]. After few days of cooling the γ dose rate is dominated by ^{7}Be and the β dose rate by ^{14}C, both of which are radiologically relatively harmless. Thus, compared to the aluminium, silicon and steel elements of the Tracker, the carbon fibre structures give a negligible contribution to the dose.

Activation of the beam pipe

The activation of the beam pipe is an important issue for the Pixel maintenance and any operations on the beam pipe itself.

The installation of the Pixel detector requires work very close to the beam pipe in the region of the stainless-steel/aluminium transition. Therefore we calculate the dose in contact

[2] Tritium is produced with a large cross-section but, due to its very low β-energy, is harmless when contained in a solid material.

with ±1 m long aluminium and stainless steel tubes having radii of 2.5 cm and 7 cm and wall thicknesses of 0.2 mm. The activities are determined using experimental activation cross-sections for aluminium and iron. The results, shown in Table 6.32 indicate that the contact dose rate from the beam pipe is relatively high even after long cooling times. Because of the lower β emission the contact dose rate for a steel pipe drops below that from an aluminium pipe after about one month of cooling.

Table 6.32: Estimated contact dose rates (μSv/h) for the beam pipe after 10 years of LHC operation. The β-dose rate estimate corresponds to the skin surface. Dose rates from aluminium and steel (iron) are compared

Position	Dose type	t_c=1 day	t_c=7 days	t_c=30 days	t_c=150 days
$z = 0$–167 cm 2.5 cm	γ (Al)	610	310	300	270
	γ (Fe)	3000	2200	1200	530
	β (Al)	950	380	370	340
	β (Fe)	1800	860	230	58
$z = 400$–470 cm 7.0 cm	γ (Al)	140	59	58	52
	γ (Fe)	560	420	240	110
	β (Al)	170	59	58	53
	β (Fe)	270	130	33	8

We can observe that the dose rates in contact with the beam pipe are quite high even after long cooling times. People working in the vicinity of the beam pipe will expose their whole body to the radiation; in Fig. 6.53 the estimates of the γ dose rate at various distances from a plain CMS beam pipe are shown.

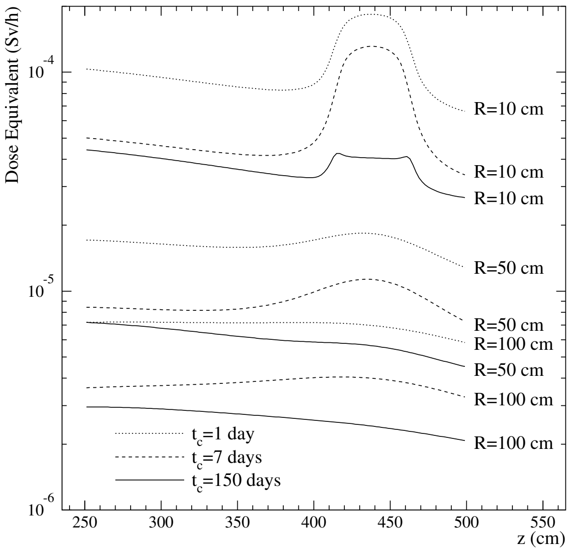

Fig. 6.53: Dose rate at various distances from the bare CMS beam pipe after the indicated cooling time t_c. Values correspond to the end of the tenth year at the LHC.

Dose equivalent rate from the whole Tracker

The preceding sections have discussed the dose rates in contact with individual pieces of the Tracker, which is required input for handling the Tracker elements. The first phase in the Tracker maintenance will be, however, to disconnect the Tracker services. This work has to be performed between the Tracker endflange and the ECAL endcap. The dose rate from the ECAL endcap has been already discussed. In this section we provide an estimate of the γ dose rate from the whole Tracker when viewed from one end flange. Due to their short range the

β's do not need to be considered. The Tracker model used for this calculation consists of two materials, silicon and carbon fibre, distributed uniformly along z. The radial distribution is fitted to reproduce the actual distribution of corresponding materials in the V4 Tracker.

The gamma spectra are calculated for these two materials as described in Section A.7.8. These gamma spectra have then been used to estimate the dose at the Tracker end-flange and around the Silicon Tracker taking attenuation in the Tracker material into account by assuming an average mass-absorption coefficient of $0.025\,\mathrm{cm^2g^{-1}}$ for all γ-energies and materials. The results are given in Fig. 6.54. The $t_c = 0$ curves are given only to indicate the fast decay of the dose during the first day. In reality access to the Tracker will be possible only a few days after LHC shut-down. It can be seen that the further decay of dose from $t_c = 1$ day to $t_c = 150$ days is relatively small. In all positions at the Tracker endflange the dose during the maintenance period is below 100 μSv/h. The highest dose, observed at small radii, is dominated by the activity in the beam pipe, which in the calculation is included up to $z = 5\,\mathrm{m}$. The middle plot of Fig. 6.54 shows the dose on the side of the Silicon Tracker with beam pipe and Pixel detector removed. During the maintenance period the dose remains below $10\,\mu$Sv/h. The time evolution, based on the assumption of the operation schedule described in Section A.5, shows that during the low-luminosity start-up phase the doses are even lower and reach saturation only towards the tenth year of operation.

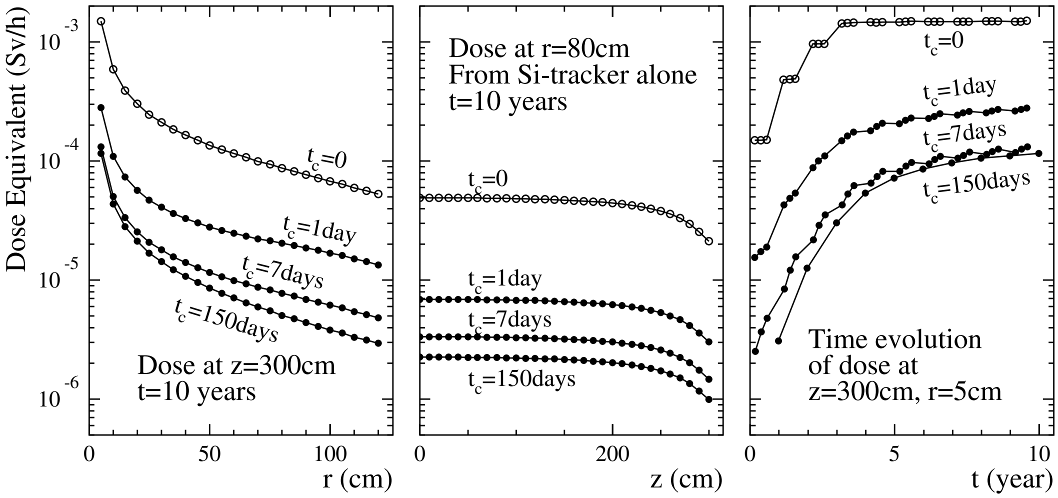

Fig. 6.54: Photon dose rate around the Tracker. The two plots on the left give the dose as a function of position after 10 years of operation for different cooling times t_c (the second curve from below corresponds to $t_c = 7$ days). The plot on the right indicates the time evolution of the dose. The open symbols are based on radionuclide yields from FLUKA directly, the solid ones are based on experimental data.

The slow decay of the activity is due to the fact that, after the first days of cooling, ^{22}Na – with its half-life of 2.6 years – remains as the only significant isotope. A comparison of the values given in Figs. 6.51 and 6.54 shows that the ECAL gives a significant contribution to the dose at the Tracker endflange. The actual dose will depend on the geometry during maintenance, in particular the amount of retraction of the endcap. At the lowest corner of the ECAL, however, the dose rate is so high that some special maintenance time shielding will have to be installed. This shielding will also reduce the dose which people working at the Tracker end flange will receive.